International Journal of Modern Manufacturing Technologies
ISSN 2067–3604, Vol. XIV, No. 3 / 2022
https://doi.org/ 10.54684/ijmmt.2022.14.3.319

THERMOELASTIC DISPLACEMENT DUE TO TRANSIENT SURFACE HEATING

Delia Cerlinca[1,2], **Sergiu Spinu**[1,2]

[1] Department of Mechanics and Technologies, Stefan cel Mare University of Suceava,
13th University Street, 720229, Romania
[2] Integrated Center for Research, Development and Innovation in Advanced Materials, Nanotechnologies, and Distributed Systems for Fabrication and Control (MANSiD), Stefan cel Mare University, Suceava, Romania

Corresponding author: Sergiu Spinu, sergiu.spinu@fim.usv.ro

Abstract: The starting point in the calculation of normal displacement due to transient heating is the Green's function for the elastic half-space. Superposition principle leads to a triple integral (double integral over surface and simple integral over time) that can be formally re-written as a three-dimensional convolution product. Given the singularities of the Green's function in the time/space domain, it is more convenient to employ its spectral counterpart, i.e. the frequency response function (FRF), in the convolution calculation. A special technique for the calculation of the 3D convolution product based on the FRF is advanced in this paper. The resulting algorithm is very efficient from a computational point of view, as the transfers to and from the time/space domain to the frequency domain are handled by the fast Fourier transform. A simulation example is presented, involving the transient thermoelastic displacement due to a uniform heat source that vanishes everywhere except for a square surface domain, and which is applied continuously only in a limited time window. The numerical results predict that the displacement increases with time as long as heat is supplied, and is gradually recovered once the heat is removed. The loaded half-space patch undergoes a growth-release process that is accurately captured by the simulation method. The developed framework anticipates the solution of the contact process with transient heating.
Key words: thermoelastic displacement, transient heat, three-dimensional convolution, fast Fourier transform.

1. INTRODUCTION

The relative motion of the contacting surfaces in a mechanical contact causes frictional heating and thermoelastic displacements that modify the contact geometry and therefore disturb the pressure distribution computed according to an isothermal contact model. Whereas in some situations the heat generation can be assumed as a steady-state process, transient surface heating is more challenging from the point of view of model complexity, but in the same time more realistic for engineering scenarios.

Many dependencies in engineering systems can be expressed as convolution products. Finding a way to numerically compute convolutions for arbitrary input has been the subject of important research efforts, especially in Contact Mechanics, in which the number of analytical solutions is limited to a few.

The efficient calculation of a convolution product supports the development of iterative schemes for problems that lack analytical solutions. With the rapid calculation of convolutions, engineering scenarios considered otherwise unsolvable due to prohibitive computational effort found rapid solution through numerical approach assisted by the spectral methods. At the heart of these methods stand the convolution theorem and the fast Fourier transform (FFT), which is a very efficient algorithm to calculate the discrete Fourier transform. Review papers of the various applications of the FFT in Contact Mechanics can be found in [1,2]. The pioneering works of Ju and Farris [3] and of Ju and Farris [4] anticipated the method potential for both contact problems and thermoelastic solutions for moving heat sources. Their work was continued and extended in numerous directions. Various methods for numerical simulation of the mechanical contact were advanced [5-12], capitalising on the method ability to speed up the displacement calculation. The stress calculation in elastic half-spaces, either homogeneous or in the presence of eigenstrains, also benefitted [13-15] from FFT integration and support.

Another important application of FFT is in thermoelastic modelling. Liu et al. [16] advanced a fast method for the computation of the normal surface displacement due to arbitrary transient surface heating. Liu and Wang [17] solved the three-dimensional thermomechanical contact of non-conforming rough surfaces. Liu et al. [18] advanced a novel set of frequency-domain functions for computation of temperature distributions and thermoelastic

displacements in moving bodies. The transient thermoelastic stress fields in a material subjected to frictional heating were studied by Liu and Wang [19]. Martini et al. [20] proposed a transient, three-dimensional solution for the normal surface displacement of an elastic half-space due to an arbitrarily distributed, moving heat source and surface convection.

This paper advances a very efficient computational method for the calculation of normal displacement at the boundary of an elastic half-space due to an arbitrary transient heat flux.

2. HEAT CONDUCTION EQUATIONS

For many engineering scenarios, solids of arbitrary profiles can be idealised as half-spaces for the calculation of the displacement field induced by surface tractions (e.g., pressure) or heat flux. This assumption is reasonable when heat is supplied to the solid over a finite area, such as the contact area established in the concentrated contact between bodies of dissimilar profiles.

Thus, the starting point in the model development is the displacement solution for a point source of heat located on the half-space boundary. Further on, due to the linearity of heat conduction equations, the body response to arbitrary distributions of heat can be found by superposition of solutions for point sources. A similar technique has been successfully applied in Contact Mechanics for the displacement due to arbitrary pressure, obtained by superposition of half-space solutions for point forces [21]. The solutions for unit point stimuli are referred to as the Green's functions, and are a counterpart of the unit impulse response in digital signal processing.

For heat conduction phenomena, the half-space assumption implies that the temperature gradients are large only in a small vicinity of the heated region, which can be considered as approximately plane. Moreover, global temperature changes in the bulk of the bodies do not significantly affect the thermal stresses and displacements in the considered heated regions. These assumptions are well adapted to concentrated contacts with frictional heating, in which the contact area that transfers heat is small, and the clearance in the non-contacting regions acts as an insulator. An elastic half-space is reported to a Cartesian coordinate system with two axes contained in its boundary and the third one pointing in the depth direction. A transient heat flux $q(x',y',t')$ applied on the surface, depending on the position on the half-space boundary (x',y') and on time t', causes a temperature rise in the half-space $\Delta T(x'',y'',z'',t)$, which in its turn leads to a displacement field $u_k(x,y,z,t)$, $k=1,2,3$, given by [16,22]:

$$u_k(x,y,z,t)=\int_0^{\infty}\int_{-\infty}^{\infty}\int_{-\infty}^{\infty}\frac{(1+\nu)\alpha\Delta T(x'',y'',z'',t)}{4\pi(1-\nu)}\left((3-4\nu)(2\delta_{3k}-1)\left(\frac{1}{R_2}\right)_{,k}-\left(\frac{1}{R_1}\right)_{,k}-2z\left(\frac{1}{R_2}\right)_{,3k}\right)dx''dy''dz''; \quad (1)$$

$$R_1^2=(x-x'')^2+(y-y'')^2+(z-z'')^2;\quad R_2^2=(x-x'')^2+(y-y'')^2+(z+z'')^2,$$

where ν is the Poisson's ratio of the half-space material, α its linear thermal-expansion coefficient, δ_{ij} the Kronecker delta, and $(f)_{,k}$ denotes the partial derivative of f with respect to the direction k, with $k=x,y$ or z.

This displacement field has components along all three directions, but for contact problems the normal displacement (i.e., aligned with the depth direction) is of interest because it dictates the shape and size of the contact area, as well as the pressure distribution. By taking $k=3$ and $z=0$ in (1), the normal displacement results as:

$$u_z(x,y,0,t)=\frac{-\alpha(1+\nu)}{\pi}\times$$

$$\times\int_0^{\infty}\int_{-\infty}^{\infty}\int_{-\infty}^{\infty}\frac{\Delta T(x'',y'',z'',t)z''}{\left((x-x'')^2+(y-y'')^2+z''^2\right)^{3/2}}dx''dy''dz''. \quad (2)$$

On the other hand, the temperature rise in the half-space $\Delta T(x'',y'',z'',t)$, caused by the heat flux $q(x',y',t)$, can be expressed as:

$$\Delta T(x'',y'',z'',t)=\frac{\kappa}{4K\pi^{3/2}}\times$$

$$\times\int_0^{t}\int_{-\infty}^{\infty}\int_{-\infty}^{\infty}\frac{q(x',y',t)}{\left(\kappa(t-t')\right)^{3/2}}e^{\frac{(x''-x')^2+(y''-y')^2+z''^2}{-4\kappa(t-t')}}dx'dy'dt', \quad (3)$$

with κ the material diffusivity, expressed in m^2/s, and K its conductivity, in $\mathrm{W}/(\mathrm{m}\cdot\mathrm{K})$. Equations (2) and (3) can be combined into a 3D convolution product relating the displacement to the heat input:

$$u_z(x,y,0,t) = \int_0^t \int_{-\infty}^{\infty} \int_{-\infty}^{\infty} q(x',y',t) \times \\ \times G(x-x',y-y',t-t')dx'dy'dt', \quad (4)$$

whose kernel (or Green's function) $G(\xi,\zeta,\Delta t)$, expressed in terms of the distortivity $d = \alpha(1+\nu)/K$ and with the substitutions $\xi = x - x'$, $\zeta = y - y'$, $\Delta t = t - t'$, takes the following form:

$$G(\xi,\zeta,\Delta t) = \frac{-d}{4\pi^{5/2}\kappa^{1/2}\Delta t^{3/2}} \int_0^{\infty} \int_{-\infty}^{\infty} \int_{-\infty}^{\infty} \frac{z''}{\left[(x-x'')^2 + (y-y'')^2 + z''^2\right]^{3/2}} e^{\frac{(\xi-x+x'')^2+(\zeta-y+y'')^2+z''^2}{-4\kappa\Delta t}} d\xi d\zeta dz''. \quad (5)$$

From a computational point of view, the classic evaluation of (4) and (5) implies the treatment of singularities by truncation of convergent series [23]. The convolution calculation in the frequency domain may present itself as a more convenient approach. To this end, Liu et al. [16] have expressed analytically the Fourier domain counterpart of equation (4), by taking the triple Fourier transform (FT) of each term. If $(\omega_x, \omega_y, \omega_t)$ are the angular frequencies for directions (x, y, t), equation (4) takes the following form in the frequency domain:

$$\tilde{\tilde{\tilde{u}}}_z(\omega_x,\omega_y,0,\omega_t) = \tilde{\tilde{\tilde{q}}}(\omega_x,\omega_y,\omega_t) \cdot \tilde{\tilde{\tilde{G}}}(\omega_x,\omega_y,\omega_t), \quad (6)$$

in which each "~" symbol denotes the application of FT to a dimension, amounting to two space dimensions and one temporal dimension. It should be noted that, when transferred to the frequency domain, a convolution operation reduces to a simpler element-wise product, according to the convolution theorem. This remarkable feature suggests to perform the numerical calculation of (6) instead of (4). Although computation of (6) require the additional transfer of the convolution terms to the frequency domain, and of the convolution result from the frequency domain back to the space/time domain, it is still the more convenient method. For the general case (referred to as transient - instantaneous in [16]), when:

$$q(x',y',t') = \delta(x')\delta(y')\delta(t'), \quad (7)$$

with δ the Dirac delta function, the Fourier transform of the Green's function, also known as the frequency response function (FRF), can be expressed as:

$$\tilde{\tilde{\tilde{G}}}(\omega_x,\omega_y,\omega_t) = \frac{2di\kappa}{\omega_t}\left[1 - w\left(\sqrt{\frac{i\omega_t}{\kappa} + w^2}\right)^{-1}\right], \quad (8)$$

where $w^2 = \omega_x^2 + \omega_y^2$ and $i^2 = -1$. It should be noted that, for the steady-state case, when the heat flux does not depend on time, i.e., $q = q(x',y')$, but $q \neq q(t')$, by taking the limit $t' \to \infty$, the FRF (as a function of the spatial coordinates) becomes:

$$\tilde{\tilde{G}}(\omega_x,\omega_y) = -d/w^2, \quad (9)$$

which is consistent with other analytical results from the literature [21].

A computationally efficient method for the evaluation of the three-dimensional convolution (4) through the element-wise product (8), based on the convolution theorem and on the FRF (8), is presented in the following section.

3. COMPUTATIONAL TECHNIQUE

The main idea of the proposed method stems from the convolution theorem, which states that a convolution in the time/space domain, in this case the one given by equation (4), can be evaluated in the frequency domain by the multiplication of the transformed convolution terms, as shown by equation (6). The calculation result is first obtained in the frequency domain, but can then be transferred back to the time/space domain, where the rest of the problem model is solved. The multiplication in the equation (6) is clearly less computationally intensive than the convolution itself, but additional calculation effort is needed to obtain the Fourier transforms of *q* and *G*, as well as the inverse Fourier transform of $\tilde{\tilde{\tilde{u}}}_z$.

As the goal of this paper is to achieve a method capable of displacement calculation for arbitrary heat input, numerical methods are employed. The continuous problem model is substituted by a discrete one. As equation (4) relates the surface displacement output u_z directly to the heat input *q*, which is also a surface parameter, only a two-dimensional grid is needed in the half-space boundary, encompassing the (surface) region through which heat is supplied. In order to benefit from the computational advantages of the spectral methods, the imposed grid must be rectangular and uniform (although the step can be different in magnitude from one dimension to the other).

For every elementary patch, a single scalar is retained, so that every continuous model parameter is substituted by an array, i.e., a piece-wise constant approximation of continuous distributions. In case of equation (4), the convolution terms *q* and *G* depend on two spatial dimensions and on one temporal dimension, thus their discrete counterparts are three-dimensional arrays. Thus, although the spatial grid is only two-dimensional (a surface grid), the transient model feature adds the time dimension, and the convolution becomes three-dimensional. If $N = N_x N_y N_t$ is the total number of discrete points in the time-space discretization, the computational effort for the calculation of convolution in the time/space domain by classic computation of (4) is of order $O(N^2)$, whereas equation (6) amounts to a more convenient $O(N)$, to which the cost of the transfer to and from the frequency domain must be added. The latter cost is of order $O(N \log N)$ when using performant algorithms such as the fast Fourier transform (FFT). Applying FFT to three-dimensional array is straightforward and involves computing the one-dimensional transform along each of the three dimensions. Thus, the global advantage of convolution calculation in the frequency domain according to relation (6) is a reduction from $O(N^2)$ to $O(N \log N)$.

Aliasing issues affecting the calculation result were observed [13] when the described method was applied in the calculation of displacement due to an arbitrary pressure input. A more in-depth analysis of the method error was conducted [13]. A so-called periodicity error was identified when discretization and FFT were applied to non-periodic problems. The error source is the implicit assumption taken when FFT is applied to a discrete series, that the series comes from a periodic distribution. Practically, the convolution calculation in the frequency domain is the result of periodical distributions, which may affect precision as the computed output also contains contributions from the neighboring spurious periods of the input. Various methods were proposed [5,7-9,12] to reduce and control this method error.

The algorithm proposed in this paper takes advantage of state-of-the-art techniques for FFT application to Contact Mechanics, reviewed in [2]. The algorithm flow-chart consists in the following steps:

1. Establish the mesh parameters in the time/space domain, i.e., the domain lengths L_x, L_y, L_t, resulting in the mesh intervals $\Delta_m = L_m / N_m$, with $m = x, y, t.$

2. The reduction of aliasing in the frequency domain implies an increase of the resolution in the frequency domain, which can be achieved by extending the domain lengths L_x, L_y, L_t, while keeping the mesh intervals constant. The side lengths in the extended domain are $\bar{L}_m = \beta L_m$, $m = x, y, t,$ whereas the numbers of grids increase accordingly $\bar{N}_m = \beta N_m$ to conserve the step intervals. By numerical experimentation, the interval for the recommended β value is between 4 and 12.

3. Generate the mesh in the frequency domain, associated to the mesh in the time/space domain. The Fourier domain in each direction is centred around origin (zero frequency) and has a length of $2\pi/\Delta_m$, while the mesh interval is $2\pi/L_m$, with $m = x, y, t.$

4. Obtain a discrete approximation of the FRF by evaluating expression (8) in each point of the frequency domain grid. The result is a three-dimensional array ϕ_{ijk}, with $i = 1 \ldots \bar{N}_x$, $j = 1 \ldots \bar{N}_y$, $k = 1 \ldots \bar{N}_t$, that replicates in the frequency domain, the convolution term related to the Green's function. It should be noted that this method bypasses integration of the Green's function (5), which exhibits singularities and has infinite limits for integration.

5. Acquire (or discretize) the heat input in the initial domain, obtaining a three-dimensional array q_{ijk}, $i = 1 \ldots N_x$, $j = 1 \ldots N_y$, $k = 1 \ldots N_t$. Add zeroes (also known as zero-padding) in all directions to express the heat input in the extended domain, $\bar{q}_{ijk}$, $i = 1 \ldots \bar{N}_x$, $j = 1 \ldots \bar{N}_y$, $k = 1 \ldots \bar{N}_t$.

6. Apply FFT to $\bar{q}_{ijk}$ three times (in each direction), resulting in a counterpart in the frequency domain φ_{ijk}, $i = 1 \ldots \bar{N}_x$, $j = 1 \ldots \bar{N}_y$, $k = 1 \ldots \bar{N}_t$:

$$\phi = FFT(FFT(FFT(\bar{q}))) . \qquad (10)$$

7. Obtain the Fourier transform of displacement γ by element-wise product, according to equation (6):

$$\gamma_{ijk} = \phi_{ijk} \cdot \varphi_{ijk} , \; i = 1 \ldots \bar{N}_x, j = 1 \ldots \bar{N}_y, k = 1 \ldots \bar{N}_t . \qquad (11)$$

8. Obtain the displacement in the time/space domain by inverse FFT applied in the three dimensions:

$$u = IFFT(IFFT(IFFT(\gamma))) . \qquad (12)$$

The three-dimensional array of displacement values obtained from (12) has $\bar{N}_x \bar{N}_y \bar{N}_t$ elements (matching the extended computational domain), but precision is guaranteed only for the central $N_x N_y N_t$ values, corresponding to the initial target domain.

Discretization of the FRF in step 4 of the proposed algorithm involves singularities when evaluating in the

origin of the frequency domain for the time angular frequency, i.e., when $\omega_t = 0$. For the investigated problem, the entire slice $\omega_t = 0$, i.e., a matrix with $\bar{N}_x \bar{N}_y$ elements, cannot be computed by direct substitution of discrete frequencies $(\omega_x, \omega_y, \omega_t = 0)$ into relation (8). Such singularities were also found in the contact problem of layered materials, and were dealt with in the following manner [5,13]: the missing samples were substituted by the average value of the FRF over the elementary patch on which the singularity was encountered.

This approach relies on numerical integration to find the three-dimensional integral of the FRF over an elementary cuboid of side lengths equal to the mesh steps in the frequency domain, thus having a volume $V = (2\pi/L_x)\cdot(2\pi/L_y)\cdot(2\pi/L_t)$. Consequently, the samples in the matrix corresponding to the slice $\omega_t = 0$ should be calculated as:

$$\phi_{ijk} = \frac{\int_{t\ell}^{tu}\int_{y\ell}^{yu}\int_{x\ell}^{xu} \tilde{\tilde{G}}(\omega_x', \omega_y', 0)\, d\omega_x' d\omega_y' d\omega_t'}{V}, \qquad (13)$$

where $t\ell = -\pi/L_t$, $tu = -t\ell$, $x\ell = (\omega_x)_i - \pi/L_x$, $xu = (\omega_x)_i + \frac{\pi}{L_x}$, $y\ell = (\omega_y)_j - \frac{\pi}{L_y}$, $yu = (\omega_y)_j + \frac{\pi}{L_y}$; $(\omega_x)_i$ and $(\omega_y)_j$ are the discrete frequencies corresponding to the (i, j) element in the 2D matrix (slice) corresponding to $\omega_t = 0$. Matlab function *integral3* exhibited no convergence issues with the default absolute and relative tolerance parameters and with $\beta = 8$ in all three dimensions. This method of substitution was demonstrated [5,13] to have a high precision and therefore was implemented in the current method as well.

A calculation example of the displacement induced by a transient heat flux is reported in the following section.

4. SIMULATION EXAMPLE

The transient thermoelastic displacement caused by a uniformly distributed heat source is simulated with the proposed numerical technique. The heat source is of type (7) (i.e. transient – instantaneous). In order to neglect the material thermoelastic properties, which are material constants, displacement is normalized by the distortivity d and time by the diffusivity κ. As this is an academic calculation example, the units of measurements will be omitted for brevity. The heat source is released in a normalized time period, and vanish everywhere except inside a square:

$$q = \begin{cases} 1, & \text{if } (-2 \le x \le 2)\cdot(-2 \le y \le 2)\cdot(0 \le \kappa t \le 0.5) \\ 0, & \text{otherwise} \end{cases} \qquad (14)$$

The simulation domain is a cuboid of side lengths $8\times8\times1$, where the first two dimensions are for spatial localization and the third one for time, i.e., $0 \le \kappa t \le 1$. A uniform mesh is established in the latter domain, and the convolutions calculations in the frequency domain are performed with an 8 times increase of resolution in the frequency domain, thus $\beta = 8$ in step 2 of the algorithm.

The two-dimensional displacement fields predicted for $\kappa t = 0.5$, i.e., when the heat source is removed, and for $\kappa t = 1$, i.e., at the end of the simulation window, are depicted in figures 1 and 2. The variation of displacement along the x-direction with time is depicted in figure 3. Only half of the spatial domain was retained due to problem symmetry with respect to the y-direction.

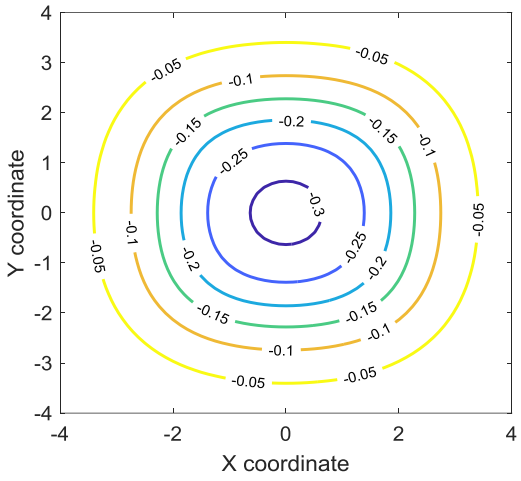

Fig. 1. Iso-contours of the displacement field $u/(2d)$ predicted for $\kappa t = 0.5$.

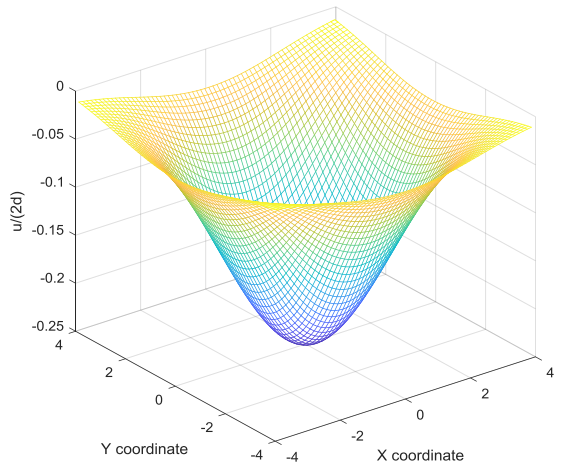

Fig. 2. The displacement field predicted for $\kappa t = 1$ (the end of the simulation window).

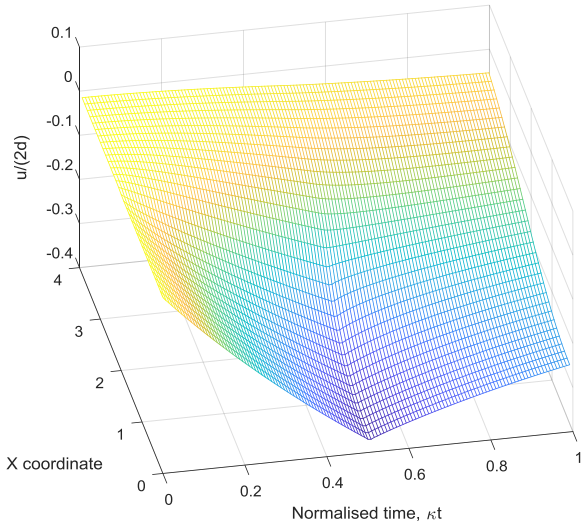

Fig. 3. Displacement profiles along *x*-coordinate, as a function of time.

As the *z*-direction of the Cartesian coordinate system was chosen to point into the half-space, the negative sign of displacemement suggests that the half-space grows when heat is liberated at its boundary, which is consistent with the general theory of heat conduction. The protuberance increases with time as long as heat is supplied. When the heat is released at $\kappa t = 0.5$, the growth process stops and the deformation is gradually recovered, but extends beyond the limit of simulation window at $\kappa t = 1$.

This example shows the method ability to replicate the transient displacement of a half-space due to arbitrary transient heat. Integration with other engineering problems such as the mechanical contact with frictional heating is intended for future studies.

5. CONCLUSIONS

This paper advances a numerical method for the calculation of transient thermoelastic normal displacement due to arbitrary heat input liberated at the half-space boundary. The method employs heat conductions equations derived in the Fourier transform domain, which are simpler to handle computationally than their time/space domain counterparts. The convolution theorem brings additional computational gains, by replacing the computationally intensive convolution product in the time/space domain with a simple product in the frequency domain. Whereas previous applications of the convolution theorem to normal displacement calculation resulted in two-dimensional convolutions, the transient model feature adds the temporal dimension, resulting in a three-dimensional convolution.

The algorithm uses the analytical frequency response functions derived in the literature, and bypasses tedious integration of the Green's functions in the time/space domain. Singularities in the frequency domain are handled by replacing the missing samples with the mean value of the frequency response function on the attached elementary domains.

A simulation example predicts the transient thermoelastic displacement due to a square heat flux transferred in a limited time window. The numerical results show the growth-release progression of the heated half-space boundary.

The derivation of this method is expected to enable the study of the mechanical contact while dealing with complicated transient thermomechanical effects.

6. REFERENCES

1. Wang Q. J., Chen W. W., Liu S., (2007), *Tribological modeling: Application of fast Fourier transform*, Tribol. Int., 40(8), 1284-1293.

2. Wang Q. J., Sun L., Zhang X., Liu S., Zhu D., (2020), *FFT-Based methods for computational contact mechanics*, Front. Mech. Eng., 6, 61.

3. Ju F., Farris T. N., (1997), *Spectral analysis of two-dimensional contact problems*, ASME J. Tribol., 118, 320-328.

4. Ju F., Farris T. N., (1997), *FFT thermoelastic solution for moving heat sources*, ASME J. Tribol., 119, 156-162.

5. Nogi T., Kato T., (1997), *An FFT-based method for roughness surface contact*, ASME J. Tribol., 119, 493-500.

6. Stanley H. M., Kato T., (1997), *Influence of a hard surface layer on the limit of elastic contact-Part I: Analysis using a real surface model*, ASME J. Tribol., 119, 481-485.

7. Ai X. L., Sawamiphakdi K., (1999), *Solving elastic contact between rough surfaces as an unconstrained strain energy minimization by using CGM and FFT techniques*, ASME J. Tribol., 121, 639-647.

8. Liu S. B., Wang Q., Liu G., (2000), *A versatile method of discrete convolution and FFT (DC-FFT) for contact analyses*, Wear, 243(1–2), 101–110.
9. Polonsky I. A., Keer L. M., (2000), *Fast methods for solving rough contact problems: A comparative study*, ASME J. Tribol., 122, 36–41.
10. Chen W. W., Liu S., Wang Q. J., (2008), *Fast Fourier Transform based numerical methods for elasto-plastic contacts of nominally flat surfaces*, ASME J. Tribol., 75, 011022.
11. Zhang X., Wang Q. J., (2019), *A SAM-FFT based model for 3D steady-state elastodynamic frictional contacts*, Int. J. Solids Struct., 170, 53-67.
12. Sun L., Wang Q. J., Zhang M., (2021), *Discrete convolution and FFT modified with double influence-coefficient superpositions (DCSS–FFT) for contact of nominally flat heterogeneous materials involving elastoplasticity*, Comput. Mech., 67, 989-1007.
13. Liu S., Wang Q., (2001), *Studying contact stress fields caused by surface tractions with a Discrete Convolution and Fast Fourier Transform algorithm*, ASME J. Tribol., 124, 36-45.
14. Liu S., Wang Q., (2005), *Elastic fields due to eigenstrains in a half-space*, ASME J. Appl. Mech., 72, 871–878.
15. Liu S., Jin X., Wang Z., Keer L. M., Wang Q., (2012,) *Analytical solution for elastic fields caused by eigenstrains in a half-space and numerical implementation based on FFT*, Int. J. Plast., 35, 135-154.
16. Liu S. B., Rodgers M., Wang Q., Keer L., (2001), *A fast and effective method for transient thermoelastic displacement analyses*, ASME J. Tribol., 123, 479-485.
17. Liu S. B., Wang Q., (2001), *A three-dimensional thermomechanical model of contact between non-conforming rough surfaces*, ASME J. Tribol., 123, 17-26.
18. Liu S. B., Wang Q., Rodgers M., Keer L., Cheng H. S., (2002), *Temperature distributions and thermoelastic displacements in moving bodies*, Comput. Model. Eng. Sci., 3(4), 479-485.
19. Liu S. B., Wang Q., (2003), *Transient thermoelastic stress fields in a half-space*, ASME J. Tribol., 125, 33-43.
20. Martini A., Liu S. B., Wang, (2005), *Transient three-dimensional solution for thermoelastic displacement due to surface heating and convective cooling*, ASME J. Tribol., 127(4), 750-755
21. Johnson K. L., (1996), *Contact Mechanics* (Cambridge: University Press).
22. Seo K., Mura T., (1979) *The elastic field in a half space due to ellipsoidal inclusions with uniform dilatational eigenstrains*, ASME J. Appl. Mech., 46, 568–572.
23. Barber J. R., (1972), *Distortion of the semi-infinite solid due to transient surface heating*, Int. J. Mech. Sci., 14, 377–393.

Received: April 27, 2022 / Accepted: December 15, 2022 / Paper available online: December 20, 2022 © International Journal of Modern Manufacturing Technologies